



**HAL**  
open science

# Nonlinear thermoacoustic mode synchronization in annular combustors

Jonas P. Moeck, Daniel Durox, Thierry Schuller, Sébastien Candel

► **To cite this version:**

Jonas P. Moeck, Daniel Durox, Thierry Schuller, Sébastien Candel. Nonlinear thermoacoustic mode synchronization in annular combustors. *Proceedings of the Combustion Institute*, 2018, 37 (4), pp.5343-5350. 10.1016/j.proci.2018.05.107 . hal-02135736

**HAL Id: hal-02135736**

**<https://hal.science/hal-02135736>**

Submitted on 21 May 2019

**HAL** is a multi-disciplinary open access archive for the deposit and dissemination of scientific research documents, whether they are published or not. The documents may come from teaching and research institutions in France or abroad, or from public or private research centers.

L'archive ouverte pluridisciplinaire **HAL**, est destinée au dépôt et à la diffusion de documents scientifiques de niveau recherche, publiés ou non, émanant des établissements d'enseignement et de recherche français ou étrangers, des laboratoires publics ou privés.




## Open Archive Toulouse Archive Ouverte (OATAO)

OATAO is an open access repository that collects the work of some Toulouse researchers and makes it freely available over the web where possible.

This is an author's version published in: <https://oatao.univ-toulouse.fr/23416>

**Official URL :** <https://doi.org/10.1016/j.proci.2018.05.107>

### To cite this version :

Moeck, Jonas P. and Durox, Daniel and Schuller, Thierry  and Candel, Sébastien *Nonlinear thermoacoustic mode synchronization in annular combustors*. (2018) Proceedings of the Combustion Institute, 37 (4). 5343-5350. ISSN 1540-7489

Any correspondence concerning this service should be sent to the repository administrator:

[tech-oatao@listes-diff.inp-toulouse.fr](mailto:tech-oatao@listes-diff.inp-toulouse.fr)

# Nonlinear thermoacoustic mode synchronization in annular combustors

Jonas P. Moeck<sup>a, b, \*</sup>, Daniel Durox<sup>c</sup>, Thierry Schuller<sup>c, d</sup>,  
Sébastien Candel<sup>c</sup>

<sup>a</sup> *Department of Energy and Process Engineering, Norwegian University of Science and Technology, Trondheim 7491, Norway*

<sup>b</sup> *Institut für Strömungsmechanik und Technische Akustik, Technische Universität Berlin, Berlin 10623, Germany*

<sup>c</sup> *Laboratoire EM2C, CNRS, CentraleSupélec, Université Paris-Saclay, Gif-sur-Yvette cedex 92292, France*

<sup>d</sup> *Institut Mécanique des Fluides de Toulouse, Université de Toulouse, CNRS, INPT, UPS, Toulouse 31400, France*

## Abstract

Nonlinear coupling between azimuthal and axisymmetric modes in annular combustors is studied analytically. Based on the thermoacoustic wave equation, a model featuring three nonlinearly coupled oscillators is derived. Two oscillators represent the dynamics of an azimuthal mode, and the third accounts for the axisymmetric mode. A slow-time system for the evolution of the mode amplitudes and phases is obtained through the application of the method of averaging. The averaged system is shown to accurately reproduce the solutions of the full oscillator model. Analysis of this five-dimensional dynamical system shows that a standing azimuthal mode may synchronize with an axisymmetric mode, provided that their individual resonance frequencies and growth rates are similar. This phase-coupled two-mode oscillation corresponds to the so-called slanted mode, observed in recent experiments involving an annular model combustion chamber. Quantitative conditions for the occurrence of mode synchronization are derived in terms of the growth rate ratio and a frequency detuning parameter. The analysis results are found to be consistent with experimental observations of the slanted mode.

*Keywords:* Combustion instability; Azimuthal mode; Nonlinear synchronization; Annular chamber; Slanted mode

## 1. Introduction

Thermoacoustic instabilities occur in many technical applications where heat is added through combustion, prominent examples being stationary gas turbines for power generation and aero-engines [1,2]. In simplified laboratory configurations that host a single flame, acoustic waves propagate only

---

\* Corresponding author at: Department of Energy and Process Engineering, Norwegian University of Science and Technology, Trondheim 7491, Norway.

E-mail addresses: [jonas.moeck@ntnu.no](mailto:jonas.moeck@ntnu.no),  
[jonas.moeck@tu-berlin.de](mailto:jonas.moeck@tu-berlin.de) (J.P. Moeck).

in the axial direction and the associated modes are readily obtained from elementary calculations. Combustion chambers in the applications mentioned above, however, feature an annular geometry, in which multiple flames, typically more than 10, are distributed circumferentially. These annular combustion chambers host, in addition, azimuthal modes, for which the dominant pressure variation occurs along the angular coordinate. In full-scale engines, combustion instabilities are thus often observed to couple with the lower-order azimuthal modes [3,4].

Over the last decade, azimuthal instabilities in annular chambers have been intensely studied by experimental and numerical means [5–8] and by using analytical methods [9]. Many elementary properties of azimuthal instability modes are well understood by now, particularly those pertaining to the linear dynamics, such as the degeneracy of azimuthal modes in systems with discrete rotational symmetry. The most prominent action of the nonlinear flame response is to destabilize the standing-wave pattern so that a spinning azimuthal mode is established at finite oscillation levels [10,11]. Comprehensive nonlinear analysis [12] shows more complex phenomena, such as the simultaneous existence of stable standing and spinning waves, recently observed in the form of mode hysteresis [13]. Another phenomenon specific to annular chambers and discovered recently is the occurrence of a nonlinear coupling between axisymmetric and azimuthal modes, giving rise to a slanted pattern of the perturbed flames around the combustion chamber circumference [8]. The present article is concerned with explaining the manifestation of the slanted mode based on a nonlinear thermoacoustic model.

From a more general point of view, the slanted mode is the manifestation of nonlinear mode coupling that involves synchronization of two modes with similar individual resonance frequencies. Other aspects of synchronization have recently been studied in the field of thermoacoustics [14,15], viz. forced synchronization and synchronization of different fields. However, the present case precisely corresponds to the scenario labeled as ‘mutual synchronization of self-sustained oscillators’ in the standard reference [16, Chap. 4].

From experimental and theoretical studies of thermoacoustic instabilities in longitudinal configurations, it appears that whenever two modes with different resonance frequencies are unstable at the same time, the prevailing tendency is that only one mode survives and the other is suppressed [17], or a quasi-periodic solution emerges, in which both modes oscillate with different, generally incommensurate frequencies [18,19]. Since single-burner configurations host only longitudinal modes in the low-frequency regime, two modes cannot have close resonance frequencies, unless the system features decoupled plenum and chamber modes

[20]; therefore, synchronization between different modes is less likely to occur in these systems. An annular chamber, however, has a significantly higher modal density so that it may indeed happen that two modes have similar resonance frequencies, giving rise to synchronization.

Our analysis is based on the oscillator model introduced by Noiray et al. [11] for the investigation of the effect of asymmetry on the standing–spinning mode structure. The same model was used by Ghirardo et al. [21] to explain standing modes in symmetric systems through a nonlinear mechanism involving transverse velocity fluctuations. This model is extended here to examine the coupling between an azimuthal and an axisymmetric mode, corresponding to the slanted oscillation pattern observed in previous experiments [8]. Since the azimuthal eigenspace is spanned by two mode shapes (sine and cosine or clockwise and counter-clockwise rotating), the addition of an axisymmetric mode yields a set of three oscillator equations describing the evolution of the modes in time. Because the mode shapes are orthogonal, there is no linear coupling between the oscillators. Their interaction emerges only through the cubic term and is therefore fully nonlinear. The oscillator equations and an associated slow-time system for the amplitudes and phases are derived in Section 2. Comprehensive analysis of this system is carried out in Section 3. Section 4 discusses the analytical results in view of experimental observations.

## 2. Model equations

The oscillator model we consider is similar to the one proposed by Noiray et al. [11]. However, we include an additional axisymmetric mode and focus on cases where the resonance frequency of this axisymmetric mode is close to that of the azimuthal mode. As in previous work, we start from the wave equation for the acoustic pressure with a source term associated with the unsteady heat release rate in the flames:

$$\frac{\partial^2 \tilde{p}}{\partial t^2} + \tilde{\alpha} \frac{\partial \tilde{p}}{\partial t} - \left(\frac{c}{R}\right)^2 \frac{\partial^2 \tilde{p}}{\partial \theta^2} + \omega_0^2 \tilde{p} = (\gamma - 1) \frac{\partial \tilde{q}}{\partial t}. \quad (1)$$

Here,  $\tilde{p}$  is the acoustic pressure,  $\tilde{\alpha}$  a damping coefficient,  $c$  the speed of sound,  $R$  the mean radius of the annulus,  $\theta$  the angular coordinate,  $\gamma$  the ratio of specific heats, and  $\tilde{q}$  the heat release rate. The resonance frequency of the first azimuthal mode is  $\omega_a = c/R$ . The term  $\omega_0^2 \tilde{p}$  represents the axisymmetric mode, with resonance frequency  $\omega_0$ . An axisymmetric mode has the same phase at the circumferential locations of the flames; as such, it can be a longitudinal or a Helmholtz mode. The  $\omega_0^2 \tilde{p}$  term can be motivated by the fact that application of the Laplacian to an axisymmetric mode results in a term proportional to  $\omega_0^2 \tilde{p}$ , with an additional factor that essentially scales the amplitude of this mode.

Non-dimensional variables are introduced:  $t = \tilde{t}\omega_a$ ,  $p = \tilde{p}/(\rho c^2)$ ,  $q = \tilde{q}\rho c^2\omega_a/(\gamma - 1)$ ,  $\alpha = \tilde{\alpha}/\omega_a$ ,  $\Omega = \omega_0/\omega_a$ ;  $\rho$  denotes the mean fluid density. The unsteady heat release rate  $q$  is taken to depend on the local pressure according to  $q(p) = \beta p - \kappa p^3$  [11];  $\beta$  and  $\kappa$  are positive constants. This flame response model is simple but has been used in many recent theoretical studies (e.g., Refs. [11,21]) as it encapsulates the most important nonlinear effect, viz. saturation.

We now assume a solution of the form

$$p(\theta, t) = \eta_c(t) \cos \theta + \eta_s(t) \sin \theta + \eta_0(t). \quad (2)$$

This corresponds to the expression used in Refs. [11,12,21], except the additional term  $\eta_0$ , which represents the axisymmetric mode. The  $\cos \theta$  and  $\sin \theta$  terms span the two-dimensional eigenspace of the degenerate azimuthal mode. For a spinning mode, the amplitudes of  $\eta_c$  and  $\eta_s$  are equal, and their phase difference is  $\pm \pi/2$ . A standing wave has arbitrary amplitudes but a phase difference between  $\eta_c$  and  $\eta_s$  of 0 or  $\pi$ .

The ansatz (2) is now introduced into the wave equation (1), and after projection onto the spatial basis  $\{\cos \theta, \sin \theta, 1\}$ , coupled oscillator equations for  $\eta_c$ ,  $\eta_s$ , and  $\eta_0$  are obtained:

$$\ddot{\eta}_{c/s} + \eta_{c/s} = (\beta - \alpha)\dot{\eta}_{c/s} - \frac{3}{4}\kappa \left[ (3\eta_{c/s}^2 + \eta_{s/c}^2 + 4\eta_0^2)\dot{\eta}_{c/s} + 2\eta_{c/s}\eta_{s/c}\dot{\eta}_{s/c} + 8\eta_{c/s}\eta_0\dot{\eta}_0 \right], \quad (3a,b)$$

$$\ddot{\eta}_0 + \Omega^2\eta_0 = (\beta - \alpha_0)\dot{\eta}_0 - 3\kappa \left[ (\eta_c\dot{\eta}_c + \eta_s\dot{\eta}_s)\eta_0 + (\eta_c^2/2 + \eta_s^2/2 + \eta_0^2)\dot{\eta}_0 \right]. \quad (3c)$$

Here,  $(\dot{\cdot})$  denotes a derivative with respect to time, and the damping coefficient for the axisymmetric mode,  $\alpha_0$ , has been endowed with an additional subscript to indicate that this parameter should be allowed to be generally different from those corresponding to the azimuthal mode. The damping rate depends on the spatial structure of the mode and therefore may be different for each oscillator. Conversely,  $\beta$  is a property of the flame response and thus identical for all modes/oscillators.

Damping and linear flame response gain only appear as differences in Eq. (3), corresponding to the linear growth rates of the modes. In the following, these growth rates are denoted by  $\sigma_a = \beta - \alpha$  for the azimuthal mode and  $\sigma_0 = \beta - \alpha_0$  for the axisymmetric mode. Since we wish to study the interaction of azimuthal and axisymmetric modes,  $\sigma_a$  and  $\sigma_0$  are assumed positive.

The terms in the square brackets multiplying  $\dot{\eta}_{c/s}$  in Eq. (3a,b) and  $\dot{\eta}_0$  in (3c) correspond to nonlinear damping, which will limit the amplitude growth of the respective mode at finite oscillation levels. The term  $4\eta_0^2$  will thus reduce the growth of the

azimuthal mode while the terms  $(\eta_c^2 + \eta_s^2)/2$  will damp the axisymmetric mode. This scenario promotes mode competition. Also note that in the absence of the axisymmetric mode, with  $\eta_0 = 0$ , Eq. (3a,b) are identical to the system considered by Noiray et al. [11] in the study of a pure azimuthal mode.

For a given set of parameters and initial conditions, the oscillator equations (3) can be solved numerically, but this approach does not provide much insight. We will instead apply the method of averaging [22] to the system of coupled oscillators, which allows drawing more general conclusions about the system dynamics. The solutions are assumed to be of the form

$$\eta_i = A_i(t) \cos[t + \phi_i(t)], \quad i = \{c, s, 0\},$$

where the amplitudes  $A_i$  and phases  $\phi_i$  are assumed to be slowly varying functions of time. Note that the oscillation frequency is not a priori fixed to 1 ( $\omega_a$  in dimensional variables). A small deviation from the resonance frequency of the uncoupled mode can be accommodated in the slowly varying phase term  $\phi(t)$ .

Following standard procedures [22], the evolution equations for the slowly varying amplitude and phase variables are obtained by averaging the contributions of the oscillating quantities over one period:

$$\dot{A}_i = -\langle f_i \sin(t + \phi_i) \rangle, \quad \dot{\phi}_i = -\frac{1}{A_i} \langle f_i \cos(t + \phi_i) \rangle, \quad (4)$$

where the  $f_i$  are the right hand sides of Eq. (3), and the angled brackets denote an average over one period of the uncoupled azimuthal mode. Note that a delay in the flame response model only affects the linear gain but not the structure of the averaged system [11].

There are four parameters in the oscillator system: the growth rates of the azimuthal and the axisymmetric modes  $\sigma_a$  and  $\sigma_0$ , the ratio of the oscillation frequencies  $\Omega$ , and the saturation coefficient  $\kappa$  from the nonlinear flame model. Two of these parameters can be removed through suitable rescaling. To this effect, we introduce

$$\hat{A}_i = A_i \frac{\kappa}{\sigma_0}^{1/2}, \quad \hat{\sigma} = \frac{\sigma_a}{\sigma_0}, \quad \hat{\Delta} = \frac{\Omega^2 - 1}{2\sigma_0}, \quad \tau = t\sigma_0.$$

Furthermore, the amplitude and phase evolution equations do not depend on the phase variables independently but only on their differences. We therefore introduce phase-difference variables, defined as  $\psi_{ij} = \phi_i - \phi_j$ .

Using the averaging ansatz (4), the amplitude and phase-shift evolution equations are then obtained as

$$\hat{A}'_{c/s} = \frac{\hat{A}_{c/s}}{32} 16\hat{\sigma} - 3(3\hat{A}_{c/s}^2 + 2\hat{A}_{s/c}^2 + 8\hat{A}_0^2) + \hat{A}_{s/c}^2 \cos 2\psi_{cs} + 4\hat{A}_0^2 \cos 2\psi_{c/s0}], \quad (5a,b)$$

$$\hat{A}'_0 = \frac{\hat{A}_0}{32} [16 - 3(4\hat{A}_c^2 + \hat{A}_s^2 + \hat{A}_0^2) + 2\hat{A}_c^2 \cos 2\psi_{c0} + 2\hat{A}_s^2 \cos 2\psi_{s0}], \quad (5c)$$

$$\psi'_{cs} = \frac{3}{32} [(\hat{A}_s^2 + \hat{A}_c^2) \sin 2\psi_{cs} + 4\hat{A}_0^2 (\sin 2\psi_{c0} - \sin 2\psi_{s0})], \quad (5d)$$

$$\psi'_{c0} = -\hat{\Delta} + \frac{3}{32} (\hat{A}_s^2 \sin 2\psi_{cs} + 4\hat{A}_0^2 \sin 2\psi_{c0} + 2\hat{A}_c^2 \sin 2\psi_{c0} + 2\hat{A}_s^2 \sin 2\psi_{s0}). \quad (5e)$$

Here,  $\psi_{s0} = \psi_{c0} - \psi_{cs}$ , and  $(\cdot)'$  denotes a derivative with respect to the scaled time  $\tau$ . Also note that to leading order, the first term on the right hand side of Eq. (5e) corresponds to the frequency difference between the azimuthal and the axisymmetric mode. For small amplitudes, the phases of the axisymmetric and the azimuthal modes will thus diverge at a rate equal to the frequency difference when their uncoupled resonance frequencies are not identical. However, the nonlinear terms in (5e) may compensate the frequency difference to establish a fixed phase difference between azimuthal and axisymmetric modes in case of synchronization. Furthermore, it is evident from the system (5) that coupling between the modes occurs in a purely nonlinear fashion.

In the following, we consider the system of nonlinearly coupled differential equations (5) that evolve the system state in a five-dimensional space. The advantage of studying the averaged system is that periodic and quasi-periodic solutions can be determined much easier compared to the oscillator Eqs. (3). Periodic solutions of any kind are characterized by fixed points of the averaged system, i.e.  $[\hat{A}'_c, \hat{A}'_s, \hat{A}'_0, \psi'_{cs}, \psi'_{c0}] = 0$ , with at least one of the amplitudes being non-zero. A quasi-periodic solution would be characterized by at least one of the azimuthal mode amplitudes and the axisymmetric mode amplitude being non-zero and all of the previously mentioned state variables being constant except for  $\psi_{c0}$ , which would vary linearly in time, driven by the frequency difference between the azimuthal and the axisymmetric mode. Stability of the individual periodic or quasi-periodic solutions that may exist for certain values of the parameters is also more easily determined from the averaged system. One only needs to inspect the eigenvalues of the Jacobian evaluated at the corresponding equilibrium state.

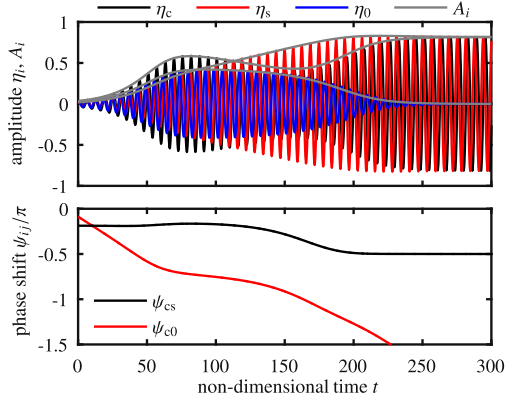


Fig. 1. Comparison of numerical solutions of the oscillator equations (3) and the averaged system (5). Top: mode coefficients  $\eta_i$  and mode amplitudes  $A_i$ ; the latter are shown as gray lines. Bottom: phase shifts from the numerical solution of the averaged system.  $\Omega = 1.03$ ,  $\sigma_a = 0.1$ ,  $\sigma_0 = 0.09$ ,  $\kappa = 0.2$ , corresponding to  $\hat{\sigma} \approx 1.11$  and  $\hat{\Delta} \approx 0.338$ .

### 3. Results, discussion, and further analysis

To assess the ability of the slow-time model (5) to represent the dynamics of the original coupled oscillator system (3), numerical solutions based on both sets of equations are compared (Fig. 1, top frame). The amplitudes from the averaged system appear as envelopes of the oscillator solutions, and it is apparent that the averaged system is a very good approximation that captures even the non-monotonic amplitude evolution accurately. The parameter values for this case are  $\Omega = 1.03$ ,  $\sigma_a = 0.1$ ,  $\sigma_0 = 0.09$ ,  $\kappa = 0.2$ , with linear growth rates and saturation coefficient chosen as in Ref. [11]. In terms of the rescaled parameters, this corresponds to a growth rate ratio  $\hat{\sigma} \approx 1.11$  and frequency detuning parameter  $\hat{\Delta} \approx 0.338$ . In the initial linear stage, all amplitudes grow exponentially because of the positive growth rates. After a transient stage with non-trivial amplitude evolution, the axisymmetric mode eventually decays to zero and cosine and sine amplitudes attain identical oscillation levels. The phase between cosine and sine modes,  $\psi_{cs}$ , settles at  $-\pi/2$  (Fig. 1, bottom), which shows that a purely spinning mode is established. Also note how the phase shift between azimuthal and axisymmetric modes, here represented through  $\psi_{c0}$ , increases linearly at small intermediate amplitudes, is nearly constant in the intermediate regime when all modes feature appreciable amplitudes, and finally drifts off when the axisymmetric mode has vanished. This indicates that the system is already close to synchronization.

Now the frequency ratio is decreased to  $\Omega = 1.01$ , corresponding to a frequency detuning parameter  $\hat{\Delta} = 0.112$  (Fig. 2). The solution of



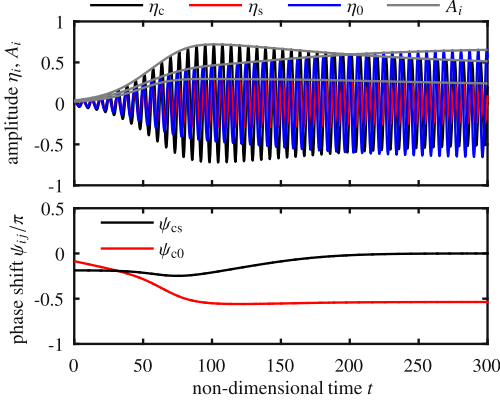


Fig. 2. As Fig. 1 but with  $\Omega = 1.01$ , corresponding to  $\hat{\Delta} \approx 0.112$ .

the averaged system again corresponds well with that of the oscillator model. In contrast to the previous case with a larger frequency detuning, all modes survive in the long-time limit and settle on constant amplitudes (visible at times larger than shown in Fig. 2). We note that the azimuthal mode is standing, indicated by  $\psi_{cs} = 0$  (Fig. 2, bottom). The amplitude ratio of the cosine and sine components determines the orientation of the nodal line of the standing azimuthal mode. In the present axisymmetric setting, all orientations are equally permissible, and it depends on the initial conditions which is established. Furthermore, the phase difference between the azimuthal and the axisymmetric mode,  $\psi_{c0}$ , settles on a fixed value, slightly less than  $\pi/2$ . A fixed phase difference  $\psi_{c0}$  implies that the two modes, which have different linear resonance frequencies, have become synchronized through the nonlinear coupling. This scenario precisely corresponds to the slanted mode documented in Ref. [8].

A phase shift close to  $\pi/2$  between azimuthal and axisymmetric modes is also observed in the averaged model and in experimental data, to be discussed in the following, and therefore appears to be a robust feature of the phenomenon. Furthermore, this phase shift is only insignificantly affected by a time delay in the flame response model, as was verified numerically on the basis of the oscillator system (3). While a delay in the flame response would generally affect the phase shift between pressure and heat release rate, the nonlinear coupling of the two modes occurs only through the pressure at the location of the flames. In the phase-locked state, both modes oscillate at the same frequency and, hence, acquire the same phase shift from the flame response; the phase shift between the modes is therefore unaffected by the delay. Similarly, a more realistic burner impedance is not expected to affect this phase shift.

In the following, we analyze the averaged system (5) to establish conditions in the reduced

parameters  $\hat{\sigma}$  (growth rate ratio) and  $\hat{\Delta}$  (frequency detuning), for which the slanted mode, i.e., the synchronized oscillation between an axisymmetric and an azimuthal mode, exists and is stable. Since there is rotational symmetry, we can assume without loss of generality that  $A_s = 0$  for a standing azimuthal mode. The amplitude Eqs. (5) then take the form

$$\hat{A}'_c = \frac{\hat{A}_c}{32} [16\hat{\sigma} - 3(3\hat{A}_c^2 + 4\hat{A}_0^2(2 + \cos 2\psi_{c0}))], \quad (6a)$$

$$\hat{A}'_0 = \frac{\hat{A}_0}{32} [16 - 3(4\hat{A}_0^2 + 2\hat{A}_c^2(2 + \cos 2\psi_{c0}))], \quad (6b)$$

with phase-difference equation

$$\psi'_{c0} = -\hat{\Delta} + \frac{3}{16} (\hat{A}_c^2 + 2\hat{A}_0^2) \sin 2\psi_{c0}. \quad (6c)$$

Since  $A_s = 0$ , the phase difference  $\psi_{cs}$  is irrelevant. For a slanted mode, the right hand sides of Eqs. (6) must vanish for non-zero  $\hat{A}_c$  and  $\hat{A}_0$ . We first determine conditions on  $\hat{\Delta}$  and  $\hat{\sigma}$  for which such solutions exist and then address the stability of the synchronized state.

From requiring that the right hand sides of Eqs. (6) vanish, an equation only involving the phase-shift variable  $\psi_{c0}$  can be obtained:

$$2(2 + \cos 2\psi_{c0})^2 - 3 \hat{\Delta} = 1/2 + \hat{\sigma} + (1 + \hat{\sigma}) \cos 2\psi_{c0} \sin 2\psi_{c0}. \quad (7)$$

This equation is quartic in  $\cos 2\psi_{c0}$  and thus may have four real solutions in any half-closed interval of length  $\pi$ . It appears that these solutions cannot be expressed in simple form for arbitrary  $\hat{\Delta}$  and  $\hat{\sigma}$ . We therefore consider first the special case where the resonance frequencies of the azimuthal and the axisymmetric mode are identical, i.e.,  $\hat{\Delta} = 0$ . Equation (7) then has the four solutions  $\psi_{c0} = \{0, \pi/2, a, -a\}$ , where  $a$  is given by  $a = \arccos[-(\hat{\sigma} + 1/2)/(\hat{\sigma} + 1)]$ , which are all modulo  $\pi$ . When these solutions are used in requiring that the right hand sides of (6a) and (6b) vanish, explicit expressions for the squared amplitudes of the two modes are obtained. The solutions  $\psi_{c0} = \pm a$  lead to negative amplitude squares for the axisymmetric mode and therefore can be discarded. With the other two solutions of the phase-shift equation (7), we obtain

$$\psi_{c0} = 0: \quad \hat{A}_c^2 = \frac{16}{45} (3 - \hat{\sigma}), \quad \hat{A}_0^2 = \frac{4}{15} (2\hat{\sigma} - 1), \quad (8)$$

$$\psi_{c0} = \frac{\pi}{2}: \quad \hat{A}_c^2 = \frac{16}{3} (\hat{\sigma} - 1), \quad \hat{A}_0^2 = \frac{4}{3} (3 - 2\hat{\sigma}). \quad (9)$$

These solutions correspond to phase coupled oscillations of an azimuthal and an axisymmetric

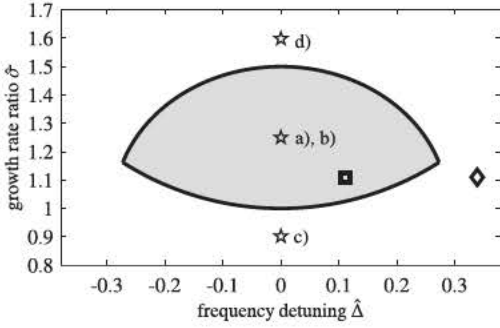


Fig. 3. Existence and stability domain (gray shaded) of the phase-coupled two-mode solution – the slanted mode – in parameter space. Stars indicate parameter combinations for which phase planes are shown in Fig. 4. Diamond and square correspond to parameters of Figs. 1 and 2, respectively.

mode, and it can be verified numerically that these are indeed equilibrium states of the full system given by Eqs. (5). Since the amplitude squares need to be positive, the conditions for the existence of a phase-coupled two-mode solution with phase shift 0 and  $\pi/2$  are  $1/2 < \hat{\sigma} < 3$  and  $1 < \hat{\sigma} < 3/2$ , respectively. As we will show later in this section, the in-phase solution with  $\psi_{c0} = 0$  is unstable so that the occurrence of a slanted mode is limited to the stricter requirement on the growth rate ratio.

When the frequencies of the two modes are not identical, i.e.,  $\hat{\Delta} \neq 0$ , the phase-shift Eq. (7) cannot be solved in simple terms. However, the range of growth rate ratios  $\hat{\sigma}$  that permits a stable phase-coupled solution can be determined numerically as a function of the frequency detuning  $\hat{\Delta}$ , as shown in Fig. 3. The effect of the frequency detuning is to reduce the range of growth rate ratios for which a slanted mode occurs. For  $|\hat{\Delta}| \gtrsim 0.273$ , no stable phase-coupled two-mode solution exists for any growth rate ratio. For a non-dimensional growth rate  $\sigma_0 = 0.2$ , this corresponds to a frequency difference of about 5%. The stability domain of the slanted mode is symmetric with respect to  $\hat{\Delta}$  because the system (6) has the symmetry  $(\hat{\Delta}, \psi_{c0}) \mapsto (-\hat{\Delta}, -\psi_{c0})$ . When  $\hat{\Delta} \ll 1$  is assumed, which is reasonable in view of Fig. 3, the effect of the frequency detuning on the phase shift can be determined to leading order from Eq. (7) as  $\psi_{c0} = \pi/2 - \hat{\Delta}$  (modulo  $\pi$ ). Hence, the azimuthal and the axisymmetric modes will always be approximately in quadrature when they are phase coupled.

It is now instructive to consider the structure of the state space defined by the system (6) to understand the qualitative changes in the stability of the synchronized two-mode solution. To this purpose, we plot the vector field defined by (6a) and (6b) corresponding to different points in the parameter space (Fig. 4a). The system is three-dimensional, and the  $\psi_{c0}$  coordinate can be thought of as

pointing out of the paper plane; however, we have already shown that only the immediate vicinity of the planes  $\psi_{c0} = 0$  and  $\psi_{c0} = \pi/2$  are of interest. Figure 4 illustrates the state space dynamics at  $\psi_{c0} = \pi/2$  for zero frequency detuning and a growth rate ratio of  $\hat{\sigma} = 1.25$ , which is most favorable for the existence of the slanted mode according to the stability map (a in Fig. 3). By construction, the origin is a repeller; the single-mode limit cycles found on the axes, where one mode has zero amplitude, both correspond to saddles: they are attracting in the direction of the non-zero mode, but repelling perpendicular to it. The in-quadrature synchronized two-mode solution is a stable node, globally attracting in the  $\psi_{c0} = \pi/2$  slice of the state space. In the slice corresponding to in-phase two-mode oscillations,  $\psi_{c0} = 0$  (Fig. 4b), the roles of the single-mode and the two-mode oscillations are reversed; the latter cannot occur as it is unstable. Also note that the single-mode oscillations are attracting only in this plane, as the phase equilibrium at  $\psi_{c0} = 0$  is unstable according to Eq. (6c).

As the growth rate ratio  $\hat{\sigma}$  is decreased from 1.25, the stable node, corresponding to the synchronized two-mode solution, successively approaches the saddle corresponding to the single-mode axisymmetric oscillation. When  $\hat{\sigma}$  is decreased below 1 (see Fig. 3), the node collides with the saddle, rendering the single-mode axisymmetric limit cycle stable (Fig. 4c). When  $\hat{\sigma}$  is increased beyond  $3/2$ , the stable two-mode oscillation collides with the single-mode azimuthal limit cycle, which is then the only stable solution (Fig. 4d). These latter effects are not entirely surprising when one recalls that  $\hat{\sigma}$  is the ratio of the growth rates of the azimuthal and the axisymmetric mode.

Only the case with zero frequency detuning is depicted in Fig. 4. However, the  $(\hat{A}'_c, \hat{A}'_0)$  vector field varies smoothly with  $\psi_{c0}$ , and the equilibrium phase shift changes only slightly with  $\hat{\Delta}$ . Qualitatively, the dynamics therefore remains similar to that shown in Fig. 4 even when  $\hat{\Delta}$  is non-zero, as long as a stable synchronized two-mode solution exists ( $|\hat{\Delta}| \lesssim 0.273$ , Fig. 3). When  $|\hat{\Delta}|$  increases beyond this value, the synchronized two-mode solution only exists as an unstable saddle, as in Fig. 4b, and the only stable solutions are single-mode limit cycles.

#### 4. Modeling results and experimental observations

The analysis in the previous section showed that the slanted mode [8] arises from a synchronization process between unstable azimuthal and axisymmetric modes. Furthermore, this synchronization is only possible when the individual resonance frequencies of the modes are close and when their growth rates are similar. This is consistent with experimental observations that the slanted mode oc-



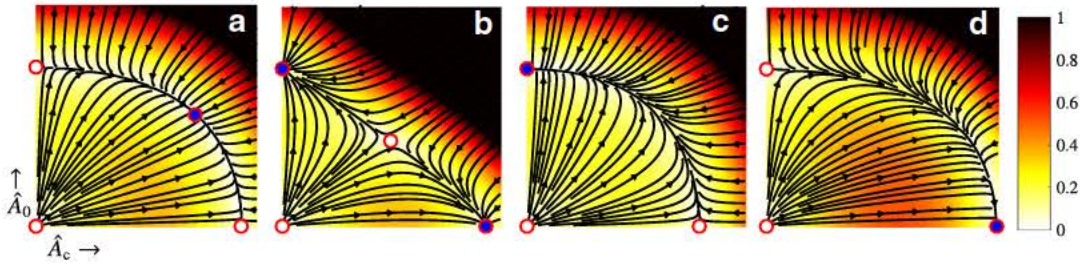


Fig. 4. Phase planes for the amplitude dynamics of the reduced standing-azimuthal-axisymmetric system, Eqs. (6a)–(6b). a)  $\hat{\sigma} = 1.25$ ,  $\hat{\Delta} = 0$ ,  $\psi_{c0} = \pi/2$ ; b)  $\hat{\sigma} = 1.25$ ,  $\hat{\Delta} = 0$ ,  $\psi_{c0} = 0$ ; c)  $\hat{\sigma} = 0.9$ ,  $\hat{\Delta} = 0$ ,  $\psi_{c0} = \pi/2$ ; d)  $\hat{\sigma} = 1.6$ ,  $\hat{\Delta} = 0$ ,  $\psi_{c0} = \pi/2$ . The amplitude range is  $\hat{A}_c = 0 \dots 1.6$  for a)–c) and  $\hat{A}_c = 0 \dots 1.7$  for d).  $\hat{A}_0$  ranges from 0 to 1.6 in all frames. Filled circles represent stable equilibrium solutions, open circles unstable ones. Background color corresponds to the norm of the amplitude rate of change,  $((\hat{A}'_c)^2 + (\hat{A}'_0)^2)^{1/2}$ ; colorscale saturates at value 1.

curs only in a very narrow region in the operating space (see Fig. 4 in Ref. [13]).

It would be interesting to test the predicted dependence of the slanted mode solution on the frequency detuning and the growth rate ratio, as illustrated in Fig. 3. This is unfortunately not possible because (i) the frequency detuning and the growth rates cannot be varied independently in the experiment, and (ii) these parameters cannot be accurately measured. However, the phase shift between the azimuthal and the axisymmetric mode,  $\psi_{c0}$ , which is predicted to be close to  $\pi/2$  from the analysis, can be retrieved from available experimental data. To this purpose, we analyze high-speed images of the flames' light emission acquired during conditions corresponding to the slanted mode (same data set as was used in Ref. [8]). The images were acquired with a Photron Fastcam APXii at a framerate of 12,000 images per second. A subset of 1000 images was analyzed by means of proper orthogonal decomposition (POD). Increasing the number of images did not noticeably affect the results presented in the following.

POD decomposes snapshots of a space and time dependent observable into orthogonal modes and ranks them according to their fluctuation energy [23]. The fluctuation energy of the first 100 modes relative to the total fluctuation energy is shown in Fig. 5. Two modes are clearly dominant, all others contributing with less than 1% to the total fluctuation energy. The first two POD modes are shown in Fig. 5 as insets. The POD mode with the largest fluctuation energy can be identified as axisymmetric thermoacoustic mode, all flames featuring the same sign of the heat release rate perturbation. In contrast, the POD mode with the second highest fluctuation energy is a first-order azimuthal mode, with positive and negative heat release rate fluctuations varying sinusoidally around the circumference. This corresponds to a standing azimuthal mode; a rotating azimuthal mode would be represented by two POD modes rotated with respect to each other by an angle of  $\pi/2$ .

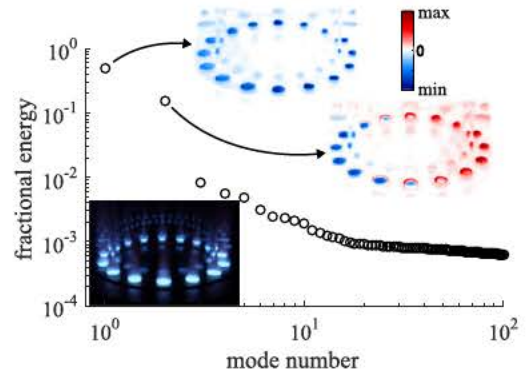


Fig. 5. Relative fluctuation energy of the first 100 POD modes obtained from high-speed imaging of the flames' light emission in the MICCA combustor when the slanted mode is observed. A long-exposure photo is shown in the inset to the lower left. The first two POD modes are shown as insets to the upper right. The light that can be seen adjacent to the actual, disk-shaped flames stems from light reflections on the quartz combustor walls.

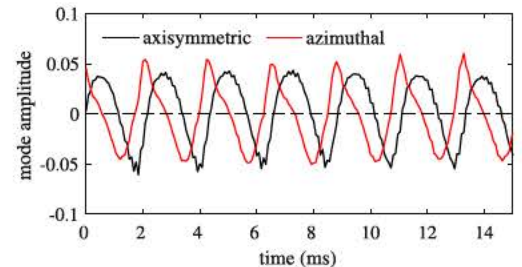


Fig. 6. Amplitudes corresponding to the axisymmetric and the azimuthal modes, obtained from POD of the high-speed images.

The phase relation of the two dominant POD modes can be deduced from their associated time coefficients. These indeed exhibit a phase shift very close to  $\pi/2$ , showing that the two modes are in quadrature (Fig. 6). The precise value of the mean

phase shift is obtained from the cross spectrum of the two time coefficients; this evaluates to 1.595 rad at the dominant frequency (450 Hz), which deviates from exact quadrature by less than 2%. This result corroborates the analysis in the preceding section, which predicted a quadrature relation whenever an azimuthal and an axisymmetric mode become synchronized in a two-mode oscillation. The instantaneous phase shift can be determined from the associated analytic signals via the Hilbert transform. This quantity shows very little deviation from the mean value, with a standard deviation of less than 0.03 rad, highlighting proper synchronization between the two modes.

## 5. Conclusion

Nonlinear coupling of thermoacoustic modes in annular combustors was investigated. A synchronized two-mode limit cycle involving a standing azimuthal and an axisymmetric oscillation, as recently observed in an annular model combustor [8], was analyzed. This phase-coupled two-mode oscillation occurs provided that the individual resonance frequencies of the two modes and their growth rates are similar. These findings were obtained by studying a reduced system that only allows for a standing azimuthal mode in addition to the axisymmetric mode. However, it can be shown that a synchronized oscillation involving a spinning azimuthal mode and an axisymmetric mode does not exist.

Through suitable rescaling, the dependence of the system dynamics on the cubic coefficient  $\kappa$ , which controls the saturation of the flame response, is removed (provided  $\kappa$  remains positive). The existence of the slanted mode solution is thus supported by a large class of flame models with saturation nonlinearity. The specific value of  $\kappa$  affects the solution on a quantitative level (the oscillation amplitude), but the analysis showed that the qualitative dynamics, i.e., single-mode oscillations or phase-locked two-mode oscillations, are unaffected. The qualitative dynamics depend only on the two non-dimensional parameters  $\hat{\sigma}$  and  $\hat{\Delta}$ , corresponding to growth rate ratio and frequency detuning, respectively. We can then expect that this nonlinearly synchronized two-mode oscillation is a rather generic feature of thermoacoustic instability in annular combustors that may appear when the

resonance frequencies and the growth rates of an azimuthal and an axisymmetric mode are close.

## References

- [1] T. Lieuwen, V. Yang, in: volume 210 of *Progress in Astronautics and Aeronautics*, AIAA, Inc., 2005.
- [2] S. Candel, *Proc. Combust. Inst.* 29 (2002) 1–28.
- [3] W. Krebs, P. Flohr, B. Prade, S. Hoffmann, *Combust. Sci. Technol.* 174 (2002) 99–128.
- [4] M. Bothien, N. Noiray, B. Schuermans, *J. Eng. Gas Turbines Power* 137 (2015) 8. 061505
- [5] G. Staffelbach, L. Gicquel, T. Poinso, *Proc. Combust. Inst.* 32 (2009) 2909–2916.
- [6] P. Wolf, G. Staffelbach, L. Gicquel, D. Müller, T. Poinso, *Combust. Flame* 159 (2012) 3398–3413.
- [7] N. Worth, J. Dawson, *Combust. Flame* 160 (2013) 2476–2489.
- [8] J.F. Bourgouin, D. Durox, J. Moeck, T. Schuller, S. Candel, *Proc. Combust. Inst.* 35 (2015) 3237–3244.
- [9] M. Bauerheim, F. Nicoud, T. Poinso, *Phys. Fluids* 28 (2016) 27. 021303
- [10] S. Stow, A. Dowling, *J. Eng. Gas Turbines Power* 131 (2009) 10. 031502
- [11] N. Noiray, M. Bothien, B. Schuermans, *Combust. Theor. Model.* 15 (2011) 585–606.
- [12] G. Ghirardo, M.P. Juniper, J.P. Moeck, *J. Fluid Mech.* 805 (2016) 52–87.
- [13] K. Prieur, D. Durox, T. Schuller, S. Candel, *Combust. Flame* 175 (2017) 283–291.
- [14] G. Penelet, T. Biwa, *Am. J. Phys.* 81 (2013) 290–297.
- [15] S.A. Pawar, A. Seshadri, V.R. Unni, R.I. Sujith, *J. Fluid Mech.* 827 (2017) 664–693.
- [16] A. Pikovsky, M. Rosenblum, J. Kurths, *Synchronization: A Universal Concept in Nonlinear Sciences*, Cambridge University Press, New York, 2001.
- [17] J. Moeck, C. Paschereit, *Int. J. Spray Combust. Dyn.* 4 (2012) 1–28.
- [18] F. Boudy, D. Durox, T. Schuller, S. Candel, *C. R. Mec.* 341 (2013) 181–190.
- [19] A. Orchini, M. Juniper, *Combust. Flame* 171 (2016) 87–102.
- [20] F. Boudy, D. Durox, T. Schuller, S. Candel, Proceedings of the ASME turbo expo, copenhagen, denmark, 11–15 june, 2012. paper no. GT2012-68998.
- [21] G. Ghirardo, M.P. Juniper, *Proc. R. Soc. Lond. A* 469 (2013) 15. 20130232
- [22] J. Sanders, F. Verhulst, *Averaging Methods in Nonlinear Dynamical Systems*, Springer-Verlag, Berlin-Heidelberg-New York-Tokyo, 1985.
- [23] G. Berkooz, P. Holmes, J. Lumley, *Annu. Rev. Fluid Mech.* 25 (1993) 539–575.